A meta-analysis of genome-wide association studies of epigenetic age acceleration

Jude Gibson[1*], Tom C. Russ[1-4], Toni-Kim Clarke[1], David M. Howard[1], Kathryn L. Evans[4,5], Rosie M. Walker[4,5], Mairead L. Bermingham[5], Stewart W. Morris[5], Archie Campbell[5,6], Caroline Hayward[7], Alison D. Murray[5,8], David J. Porteous[4,5], Steve Horvath[9,10], Ake T. Lu[9], Andrew M. McIntosh[1,4], Heather C. Whalley[1], Riccardo E. Marioni[4,5]

[1] Division of Psychiatry, Centre for Clinical Brain Sciences, University of Edinburgh, Edinburgh, UK

[2] Centre for Dementia Prevention, University of Edinburgh, Edinburgh, UK

[3] Alzheimer Scotland Dementia Research Centre, University of Edinburgh, Edinburgh, UK

[4] Centre for Cognitive Ageing & Cognitive Epidemiology, University of Edinburgh, Edinburgh, UK

[5] Centre for Genomic and Experimental Medicine, Institute of Genetics and Molecular Medicine, University of Edinburgh, Edinburgh, UK

[6] Usher Institute for Population Health Sciences and Informatics, University of Edinburgh, Edinburgh, UK

[7] MRC Human Genetics Unit, Institute of Genetics and Molecular Medicine, University of Edinburgh, Edinburgh, UK

[8] Aberdeen Biomedical Imaging Centre, University of Aberdeen, Aberdeen, UK

[9] Department of Human Genetics, David Geffen School of Medicine, Los Angeles, CA, USA

[10] Department of Biostatistics, School of Public Health, University of California-Los Angeles, Los Angeles, CA, USA

*Corresponding author

E-mail: jude.gibson@ed.ac.uk (JG)

Abstract

'Epigenetic age acceleration' is a valuable biomarker of ageing, predictive of morbidity and mortality, but for which the underlying biological mechanisms are not well established. Two commonly used measures, derived from DNA methylation, are Horvath-based (Horvath-EAA) and Hannum-based (Hannum-EAA) epigenetic age acceleration. We conducted genome-wide association studies of Horvath-EAA and Hannum-EAA in 13,493 unrelated individuals of European ancestry, to elucidate genetic determinants of differential epigenetic ageing. We identified ten independent SNPs associated with Horvath-EAA, five of which are novel. We also report 21 Horvath-EAA-associated genes including several involved in metabolism (*NHLRC*, *TPMT*) and immune system pathways (*TRIM59*, *EDARADD*). GWAS of Hannum-EAA identified one associated variant (rs1005277), and implicated 12 genes including several involved in innate immune system pathways (*UBE2D3*, *MANBA*, *TRIM46*), with metabolic functions (*UBE2D3*, *MANBA*), or linked to lifespan regulation (*CISD2*). Both measures had nominal inverse genetic correlations with father's age at death, a rough proxy for lifespan. Nominally significant genetic correlations between Hannum-EAA and lifestyle factors including smoking behaviours and education support the hypothesis that Hannum-based epigenetic ageing is sensitive to variations in environment, whereas Horvath-EAA is a more stable cellular ageing process. We identified novel SNPs and genes associated with epigenetic age acceleration, and highlighted differences in the genetic architecture of Horvath-based and Hannum-based epigenetic ageing measures. Understanding the biological mechanisms underlying individual differences in the rate of epigenetic ageing could help explain different trajectories of age-related decline.

Author Summary

DNA methylation, a type of epigenetic process, is known to vary with age. Methylation levels at specific sites across the genome can be combined to form estimates of age known as 'epigenetic age'. The difference between epigenetic age and chronological age is referred to as 'epigenetic age acceleration', with positive values indicating that a person is biologically older than their years. Understanding why some people seem to age faster than others could shed light on the biological processes behind age-related decline; however, the mechanisms underlying differential rates of epigenetic ageing are largely unknown. Here, we investigate genetic determinants of two commonly used epigenetic age acceleration measures, based on the Horvath and Hannum epigenetic clocks. We report novel genetic variants and genes associated with epigenetic age acceleration, and highlight differences in the genetic factors influencing these two measures. We identify ten genetic variants and 21 genes associated with Horvath-based epigenetic age acceleration, and one variant and 12 genes associated with the Hannum-based measure. There were no genome-wide significant variants or genes in common between the Horvath-based and Hannum-based measures, supporting the hypothesis that they represent different aspects of ageing. Our results suggest a partial genetic basis underlying some previously reported phenotypic associations.

Introduction

Ageing is associated with a decline in physical and cognitive health, and is the main risk factor for many debilitating and life-threatening conditions including cardiovascular disease, cancer, and neurodegeneration (1). Ageing is a multi-dimensional construct, incorporating physical, psychosocial, and biological changes. Everyone experiences the same rate of chronological ageing, but the rate of 'biological ageing', age-related decline in physiological functions and tissues, differs

between individuals. Various phenotypic and molecular biomarkers have been used to study biological ageing, including a number of 'biological clocks', the best known of which is telomere length. Telomeres shorten with increasing age, and telomere length has been found to predict morbidity and mortality (2). More recently, research into epigenetics – chemical modifications to DNA without altering the genetic sequence – has yielded another method for measuring biological age.

DNA methylation is an epigenetic modification, typically characterised by the addition of a methyl group to a cytosine-guanine dinucleotide (CpG) (3), that can influence gene expression and is associated with variation in complex phenotypes. This process is essential for normal development and is associated with a number of key processes including ageing. DNA methylation levels are dynamic, varying with age across the life course (4,5) and are influenced by both genetic and environmental factors (6).

Weighted averages of methylation at multiple CpG sites can be integrated into estimates of chronological age referred to as 'epigenetic age'. Two influential studies have used this method to create 'epigenetic clocks', which accurately predict chronological age in humans. Hannum et al. used DNA methylation profiles from whole blood from two cohorts to identify 71 CpG sites that could be used to generate an estimate of age (7), while Horvath used data from 51 different tissue types from multiple studies to identify 353 CpG sites whose methylation levels can be combined to form an age predictor (8). There are only six CpGs in common across the two epigenetic clocks, and they are thought to capture slightly different aspects of the biology of ageing (further details are given in **S1 Text**).

Both the Hannum and Horvath epigenetic clocks are strongly correlated ($r>0.95$) with chronological age (7,8). However, despite these high correlations, there can be substantial differences between

epigenetic and chronological age in an individual, and it is unclear what drives these differences. A greater epigenetic age relative to chronological age is commonly described as 'epigenetic age acceleration' (EAA), and implies that a person is biologically older than their years. EAA has been shown to be informative for both current and future health trajectories (9). Recently, a growing number of studies have used EAA to investigate age-related disorders, and the epigenetic clock is increasingly being recognised as a valuable marker of biological ageing (10,11).

The simplest definition of EAA is the residual that results from regressing epigenetic age on chronological age. However, it is well known that the abundance of different cell types in the blood changes with age (12,13), and hence two broad categories of EAA measures have been distinguished: those that are independent of age-related changes in blood cell composition, and those that incorporate and are enhanced by blood cell count information (10). This study focuses on two commonly used variations, based on the Horvath and Hannum epigenetic clocks, which assess different metrics to estimate biological ageing. Horvath-based epigenetic age acceleration (Horvath-EAA) is based on the CpG markers from Horvath's age predictor and is calculated such that it is independent of both chronological age and age-related changes in the cellular composition of blood. Hannum-based epigenetic age acceleration (Hannum-EAA), calculated based on the CpGs described by Hannum et al., up-weights the contributions of age-associated immune blood cells. As both the Horvath and Hannum epigenetic clocks correlate well with age, in a population with a wide age range they are guaranteed to correlate with each other. However, Horvath-based and Hannum-based epigenetic age acceleration estimates are not guaranteed to be correlated. Full details of the calculation of Horvath-EAA and Hannum-EAA are given in **S1 Text**.

Horvath-EAA, described in previous publications as 'intrinsic' epigenetic age acceleration (IEAA), can be interpreted as a measure of cell-intrinsic ageing that exhibits preservation across multiple tissues, appears unrelated to lifestyle factors, and probably indicates a fundamental cell ageing

process that is largely conserved across cell types (8,10). In contrast, Hannum-EAA, referred to in previous studies as 'extrinsic' epigenetic age acceleration (EEAA), can be considered a biomarker of immune system ageing, explicitly incorporating aspects of immune system decline such as age-related changes in blood cell counts, correlating with lifestyle and health-span related characteristics, and thus yielding a stronger predictor of all-cause mortality (10,14).

Previous studies have identified relationships between epigenetic ageing and numerous traits, including several age-related health outcomes, for example Alzheimer's disease pathology (15), cognitive impairment (15), and age at menopause (16). Higher EAA has been associated with poorer measures of physical and cognitive fitness (9) and higher risk of all-cause mortality (11). Many associations are specific to either Horvath-EAA or Hannum-EAA, a discordance that may reflect the differences in the two estimates and supports the theory that they represent different aspects of ageing (14,17,18).

While EAA has been associated with various markers of physical and mental fitness, the mechanisms underlying epigenetic ageing remain largely unknown. There has been little research conducted thus far on genetic contributions to epigenetic age acceleration. However, Lu et al. (2018) recently published results of the first genome-wide association analysis of blood EAA in a sample of 9,907 individuals, identifying five genetic loci associated with Horvath-EAA and three Hannum-EAA-associated loci (19).

This current study, with a sample size of 13,493 individuals, constitutes the largest study of the genetic determinants of DNA methylation-based ageing to date. Single nucleotide polymorphism (SNP)-based and gene-based approaches were used to identify genes and loci associated with Hannum-based and Horvath-based estimates of EAA. Functional mapping and annotation of genetic associations were performed, alongside gene-based and gene-set analyses, in an attempt to elucidate

the genes and pathways implicated in differential rates of epigenetic ageing between individuals and shed light on the underlying biological mechanisms. We report novel SNPs and genes associated with epigenetic age acceleration, and highlight differences in the genetic architectures of the Horvath-based and Hannum-based EAA measures.

Results

Estimation of epigenetic age and epigenetic age acceleration in the GS sample

A summary of the estimated epigenetic age variables is given in **Table A in S1 Data**. Both the Horvath- and Hannum-based estimates of biological age were highly correlated with chronological age (r=0.94, SE=0.005 and r=0.93, SE=0.005 respectively). The two DNA methylation age estimates were also highly correlated with each other (r=0.93, SE=0.005); however, the two estimates of epigenetic age acceleration, Horvath-EAA and Hannum-EAA, were only weakly correlated (r=0.30, SE=0.013).

GWAS of Horvath-EAA and Hannum-EAA in GS and replication of previously identified loci

The GWAS results for the Generation Scotland (GS) cohort yielded two significant ($P<5x10^{-8}$) variants for Horvath-EAA, but no SNPs achieved genome-wide significance for association with Hannum-EAA (minimum *P*-value $7.85x10^{-8}$) (**Table B in S1 Data,** full output available online at www.link_live_when_ms_accepted.com). Manhattan plots and quantile-quantile plots for the GWAS of Horvath-EAA and Hannum-EAA are shown in **Figs A and B in S2 Text**. There was a moderate genetic correlation between the two traits in the GS sample (r_G=0.597, SE=0.279), and both measures had high genetic correlations with the previously reported findings of Lu et al. (r_G=0.724, SE=0.312 and r_G=1.021, SE=0.356 for Horvath-EAA and Hannum-EAA respectively). All but one of the significant SNPs from the Lu et al. analysis of Horvath-EAA replicated (same

direction of effect and with $P<0.05$) in GS (**Table C in S1 Data**, P-value range $3.25\text{x}10^{-2}$ to $3.53\text{x}10^{-8}$). Two of the three significant SNPs from Lu et al.'s Hannum-EAA GWAS were replicated in GS (P-values $1.76\text{x}10^{-3}$ and $1.75\text{x}10^{-4}$).

GWAS meta-analysis

We conducted genome-wide association meta-analyses of Horvath-EAA and Hannum-EAA using 13,493 European-ancestry individuals aged between ten and 98 years from 12 cohorts, adjusting for sex. Manhattan plots for Horvath-EAA and Hannum-EAA are shown in **Fig 1**, with QQ plots of the observed P-values versus those expected shown in **Fig 2**. We did not find apparent evidence for genomic inflation in either the GS study (Horvath-EAA: genomic inflation factor $\lambda_{GC}=1.017$, Linkage Disequilibrium (LD) score regression intercept (SE)=1.002 (0.007); Hannum-EAA: $\lambda_{GC}=1.023$, intercept (SE)=0.998 (0.006), **Table D in S1 Data**, **Fig B in S2 Text**) or the meta-analysis (Horvath-EAA: $\lambda_{GC}=1.035$, intercept (SE)=1.006 (0.008), Hannum-EAA: $\lambda_{GC}=1.044$, intercept (SE)=1.002 (0.007), **Fig 2**); Lu et al. previously reported no evidence for genomic inflation for any of the individual studies making up their meta-analysis (19).

We identified 439 variants with a genome-wide significant association ($P<5\times10^{-8}$) with Horvath-EAA, of which ten were independent. The significantly associated variants mapped to nine genomic loci on six chromosomes (**Table 1**, full details in **Table E of S1 Data**). Of the ten independent significant variants identified here, five were novel, that is, not within ± 500 Kb of a significant variant ($P<5\times10^{-8}$) reported by Lu et al. (19). The novel findings were a SNP on chromosome 1q24.2 in the *C1orf112* gene, three SNPs on chromosome three, at 3q21.3 (nearest gene: *GATA2-AS1*), 3q22.3 in the *PIK3CB* gene, and 3q25.1 in the *LINC01214* gene, and a SNP on chromosome 12q23.3 (nearest genes: *RP11-412D9.4* and *TMEM263*). The risk alleles at these loci conferred between 0.33 (SE=0.054) and 1.34 (SE=0.127) years higher Horvath-EAA (**Table 1**). These ten independent lead SNPs showed complete sign concordance for association with Horvath-EAA

212 across GS and the Lu study (**Table F in S1 Data**). Comparing the genomic loci identified in the
213 current study with the five reported by Lu et al., only one locus that was previously reported was
214 not identified at genome-wide significance here (rs11706810 at 3q25.33, meta-analysis *P*-value
215 8.68×10^{-8}). **Figs C-L in S2 Text** show the regional association plots for the independent signals. Of
216 the ten independent SNPs achieving genome-wide significance, none associated with any other
217 phenotype in currently published GWAS available via the NHGRI-EBI catalog.

Table 1. Independent variants with a meta-analysis genome-wide significant association with Horvath-based or Hannum-based epigenetic age acceleration.

Phenotype	Index SNP	Chromosome	Position	A1/A2	Freq	Beta	SE	***P*-value**	**Gene**[a]	function	Previously reported
Horvath-EAA	rs1011267	1q24.2	169677720	A/G	0.503	-0.327	0.054	1.579E-09	*C1orf112*	intron variant	novel
	rs79070372	3q21.3	128510481	A/G	0.111	0.505	0.087	6.074E-09	*GATA2-AS1*	non coding transcript variant	novel
	rs388649	3q22.3	138777967	A/T	0.495	-0.338	0.055	6.054E-10	*PIK3CB*	intron variant	novel
	rs6440667	3q25.1	150287063	C/G	0.161	0.440	0.075	4.28E-09	*LINC01214*	intron variant	novel
	rs2736099	5p15.33	1287225	A/G	0.367	0.373	0.061	8.58E-10	*TERT*	intron variant	yes
	rs7744541	6p22.3	18104469	A/T	0.418	0.439	0.055	1.93E-15		intergenic variant	yes
	rs76244256	6p22.3	18140332	T/C	0.046	-1.341	0.127	6.231E-26	*TPMT*	intron variant	yes
	rs4712953	6p22.2	25671618	A/T	0.725	0.346	0.059	3.604E-09	*SCGN*	intron variant	yes
	rs10778517	12q23.3	106947886	T/G	0.565	0.335	0.054	4.46E-10	*RP11-412D9.4/TMEM263*	unknown	novel
	rs62078811	17q22	55031815	A/G	0.218	-0.369	0.065	1.158E-08	*STXBP4*	intron variant	yes
Hannum-EAA	rs1005277	10p11.21	37929331	A/C	0.301	0.533	0.070	2.173E-14		unknown	yes

Genome-wide significance defined as having a *P*-value of $P<5x10^{-8}$. A1 and A2 refer to the reference allele and non-reference allele for the index SNP, respectively. Freq (allele frequency), Beta (effect size), and SE (standard error of effect size) columns pertain to the reference allele, A1. Chromosome and position (in Mb) denote the location of the index SNP, and are given with regards to the GRCh38 assembly.

[a] Genes are listed if located within +/- 10 kb of a listed SNP.

The Hannum-EAA GWAS meta-analysis identified 324 genome-wide significant ($P<5\times10^{-8}$) associated variants mapping to a single genomic locus at 10p11.21 with one index SNP (**Fig 1**, **Table 1**, full details of index SNP in **Table E of S1 Data**). *ZNF25*, a transcription factor associated with osteoblast differentiation of human skeletal stem cells (20), is the closest gene to this variant, at a distance of 20 Kb. At this Hannum-EAA-related locus, the risk allele conferred 0.53 (SE=0.070) years higher Hannum-EAA. We replicated two of the three variants significantly associated with Hannum-EAA in the Lu et al. study; however, based on our clumping criteria with $r^2<0.1$, we report only one as an independent significant SNP. Conditional analysis revealed no secondary signal at this locus. The third locus reported in the previous study was not associated at genome wide significance in this larger sample ($P=3.74\text{x}10^{-3}$). A regional association plot for 10p11.21 is shown in **Fig M in S2 Text**.

Of the ten independent variants associated with Horvath-EAA, nine exhibited sign-consistent associations with Hannum-EAA, of which five attained at least nominal significance with association *P*-values less than 0.05 (most significant $P=6.9\text{x}10^{-5}$) (**Table G in S1 Data**). The single independent SNP associated with Hannum-EAA also exhibited a nominal and sign-consistent association with Horvath-EAA ($P=0.011$). Across all SNPs, however, there was little correlation between the SNP association *P*-values for the Horvath-based and Hannum-based epigenetic age acceleration measures (r=0.104, SE=0.0004, **Fig N in S2 Text**).

Heritability

Using univariate LD score regression, the SNP-based heritabilities of Horvath-EAA and Hannum-EAA were estimated to be 0.154 (SE=0.042) and 0.194 (SE=0.040) respectively (**Table D in S1 Data**), comparable to previous SNP-based heritability estimates but lower than estimates based on pedigree relationships (19).

253 **SNP functional annotation**

254 We used FUMA to functionally annotate SNPs in LD ($r^2 \geq 0.6$) with the independent significant
255 SNPs for each of the epigenetic age acceleration measures. For Horvath-EAA, this resulted in
256 functional annotation of 825 SNPs (**Table H in S1 Data**). The vast majority of the SNPs were
257 intergenic (44.85%) or intronic (47.88%), with only five (0.61%) exonic SNPs. 25 SNPs had
258 CADD scores greater than 12.37, surpassing the suggested threshold to be considered deleterious
259 and thus providing evidence of pathogenicity (21). The highest CADD scores were found in three
260 exonic SNPs: rs1800460 and rs1142345 of *TPMT* and rs10949483 of *NHLRC1* (CADD scores
261 28.40, 28.30 and 18.92 respectively), indicating potentially deleterious protein effects. Six SNPs
262 (rs413147, rs12631035, rs9851887, rs12189658, rs6915893, rs12199316) had RegulomeDB scores
263 of 1f, suggesting that variation at these SNPs is likely to affect gene expression. Almost all SNPs
264 (98.18%) were in open chromatin regions.
265
266 For Hannum-EAA, functional annotation of 1,382 candidate SNPs indicated a high proportion of
267 intergenic SNPs (60.49%), while 11.79% were intronic and only three SNPs were located in exons
268 (**Table I in S1 Data**). 14 SNPs had CADD scores above 12.37, indicating that variation at these
269 SNPs is potentially deleterious. Although 42.04% of the SNPs were located in open chromatin
270 regions, there is little evidence that the Hannum-EAA-associated locus contains regulatory regions,
271 as analysis using RegulomeDB, which integrates a larger collection of regulatory information
272 encompassing protein binding, motifs, expression quantitative trait loci (eQTLs), and histone
273 modifications as well as chromatin structure, revealed only one SNP (rs2474568) with a score
274 below 2.
275
276 **Tissue Expression analysis**
277 MAGMA (Multi-marker Analysis of GenoMic Annotation) gene property analysis linking
278 differences in epigenetic age acceleration with differences in gene expression in various tissue

types, or in brain samples of different ages and developmental stages, revealed no significant relationships after correcting for multiple tests (**Tables J-Q in S1 Data**).

Identification of expression quantitative trait loci

For the independent SNPs associated with Horvath-EAA and Hannum-EAA, evidence of eQTLs was explored using the Genotype-Tissue expression (GTEx) v7 database. Seven of the ten independent significantly associated SNPs for Horvath-EAA, and the single independent significant Hannum-EAA-associated SNP were identified as potential eQTLs (**Table R in S1 Data**). Notably, rs388649 is associated with expression of *ESYT3*, which has a role in lipid transport and metabolism pathways (22,23), expression of *FAIM*, which is associated with apoptosis and autophagy (24), in a number of skin and brain tissues, and *PIK3CB* , which regulates vital cell functions including proliferation and survival (25,26). rs76244256, the variant most strongly associated with Horvath-EAA, shows eQTL evidence for *NHLRC1* expression, which is associated with glycogen metabolism (27), across multiple tissues. The Hannum-EAA-associated SNP, rs1005277, affects the expression of several zinc finger proteins involved in transcriptional regulation (28).

Gene-based analysis

MAGMA v1.6 was used to identify gene-level associations with each EAA measure. SNPs were mapped to 17,798 protein coding genes, with genome-wide significance defined at P=0.05/17,798=2.809x10^{-6}. A total of 21 genes attained genome-wide significance for association with Horvath-EAA (**Table 2**, full details in **Table S in S1 Data**). As expected, many of these genes were located in the same regions as the lead SNPs. Three genes at 6p22.3, *NHLRC1*, *TPMT,* and *KDM1B*, had the lowest *P*-values of 1.251x10^{-23}, 4.639x10^{-23}, and 7.68x10^{-11} respectively; all these genes are involved in metabolism-related pathways (27,29,30). Although containing no genome-wide significant SNPs, 3q25.33 appears to be an important genomic region for Horvath-EAA, with

four significantly associated genes including *TRIM59* and *KPNA4*, which play roles in the immune system (31,32). Two further significant genes are *FAIM* and *TERT*, whose functions include apoptosis and autophagy (24), and telomere length-associated ageing and apoptosis (33,34) respectively. Twelve genes were significantly associated with Hannum-EAA (**Table 2**, **Table S in S1 Data**). Genes of interest include *MTRNR2L7*, a neuroprotective and anti-apoptotic factor (35,36), and *TRIM46* and *MUC1*, both located at 1q22, and which are involved with innate immune system pathways (31,37). The 4q24 cytogenetic band houses several genes significantly associated with Hannum-EAA: *MANBA* and *UBE2D3* have metabolic and innate immune system functions (23,38) while *CISD2* regulates autophagy and is involved in life span control (39,40). Comparing the results of the gene-based association analyses of Horvath-based and Hannum-based EAA, there was no overlap, and the correlation between gene-based association *P*-values for Horvath-EAA and Hannum-EAA was low (r=0.117, SE=0.007, **Fig O in S2 Text**). Manhattan plots and QQ plots for the gene-based analysis of both epigenetic age acceleration measures are shown in **Figs P and Q in S2 Text**.

319 **Table 2. Results of MAGMA gene-based association analysis for Horvath-based and Hannum-based epigenetic age acceleration.**
320

Phenotype	Gene	Chr	N_SNPs	*P*-value	Function/related pathways
Horvath-EAA	*SELP*	1	148	1.6883E-07	Immunoglobulin E responsiveness
	EDARADD	1	516	4.2627E-07	Innate immune system, cytokine signalling in immune system
	GATA2	3	72	1.0663E-07	Stem cell maintenance and hematopoietic development
	ESYT3	3	93	6.5973E-07	Metabolism, lipid transport
	CEP70	3	164	1.0891E-06	Organelle biogenesis and maintenance
	FAIM	3	49	2.4177E-08	Apoptosis and autophagy; regulates B-cell signalling and differentiation
	PIK3CB	3	175	2.52E-08	Coordinates cell functions e.g. proliferation, survival, migration
	IFT80	3	150	1.2622E-07	Organelle biogenesis and maintenance; intraflagellar transport
	SMC4	3	77	9.8909E-07	Changes in chromosome structure during mitotic segregation
	TRIM59	3	105	1.7737E-07	Multifunctional regulator for innate immune signalling pathways
	KPNA4	3	104	2.9437E-07	Cytokine signalling in immune system; protein transporter activity
	TERT	5	90	4.0455E-08	Roles in ageing and apoptosis; regulation of telomerase.
	NHLRC1	6	76	1.2512E-23	Clearance of toxic polyglucosan and protein aggregates; metabolism pathways
	TPMT	6	151	4.6385E-23	Drug metabolism - cytochrome P450; thiopurine S methyltransferase activity
	KDM1B	6	248	7.6758E-11	Metabolism of proteins, regulates histone lysing methylation
	SCGN	6	202	3.8379E-10	Calcium binding protein; neuroscience, Ca, cAMP and lipid signalling pathways
	TMEM72	10	123	1.1154E-06	Transmembrane protein
	RFX4	12	299	9.4786E-07	Transcriptional regulatory network in embryonic stem cell
	RIC8B	12	155	1.0988E-06	Can activate some G-alpha proteins; odorant signal transduction.
	C12orf23/TMEM263	12	98	6.321E-09	Transmembrane protein
	ZNF70	22	79	2.7934E-06	Transcriptional regulation; gene expression pathways
Hannum-EAA	*TRIM46*	1	27	2.66E-06	Innate immune system; cytokine signalling in immune system
	MUC1	1	15	7.33E-07	Cytokine signalling in immune system; bacterial infections in CF airways
	MANBA	4	190	1.31E-06	Glycosaminoglycan metabolism; innate immune system
	UBE2D3	4	154	1.19E-06	Metabolism of proteins; innate immune system
	CISD2	4	54	1.18E-06	Regulator of autophagy; life span control; glucose/energy metabolism pathways

	SLC9B1	4	217	2.56E-06	Sperm motility and fertility, ion channel transport
	MTRNR2L7	10	52	5.20E-07	Neuroprotective and antiapoptotic factor
	ZNF248	10	204	2.22E-07	Transcriptional regulation; gene expression pathways
	ZNF25	10	99	1.23E-08	Transcriptional regulation; gene expression pathways
	ZNF33A	10	159	8.29E-09	Transcriptional regulation; gene expression pathways
	ZNF37A	10	146	3.79E-10	Transcriptional regulation; gene expression pathways
	DNTT	10	131	2.51E-07	DNA double-strand break repair; hematopoietic cell lineage

321

322 Genome-wide significant results after Bonferroni correction for multiple testing ($P<2.809\text{x}10^{-6}$) are reported. N_SNPs is the number of SNPs in the gene.

323 **Gene-set and pathway analysis**

324 Using a competitive test of enrichment implemented in MAGMA v1.6, we did not identify any gene
325 sets that were significantly associated with either Horvath-EAA or Hannum-EAA after Bonferroni
326 correction for multiple testing. **Tables T and U in S1 Data** show the top 100 gene-sets for Horvath-
327 EAA and Hannum-EAA respectively.

328

329 **Genetic correlations**

330 The SNP-based genetic correlation between Horvath-EAA and Hannum-EAA in the meta-analysis
331 dataset, determined using LD score regression, was 0.571 (SE=0.132, P=1.605x10^{-5}), suggesting a
332 moderate overlap in the genetic factors influencing these two measures of epigenetic age
333 acceleration. We also explored genetic correlations between Horvath-EAA/Hannum-EAA and 218
334 other health and behavioural traits using LD score regression analysis of summary-level data,
335 implemented in the online software LD Hub (41). None of these phenotypes had a significant
336 genetic correlation (P_{FDR}<0.05) with either Horvath-EAA or Hannum-EAA after applying false
337 discovery rate correction (most significant correlation with Horvath-EAA: father's age at death,
338 P_{FDR}=0.160; with Hannum-EAA: waist-to-hip ratio, P_{FDR}=0.065). This correction, however, may be
339 overly conservative, as not all the tested traits are independent, with several being identical or
340 highly correlated, and nominally significant correlations ($P_{uncorrected}$<0.05) were found with a
341 number of traits (**Table 3**).

342 **Table 3. Nominally significant genetic correlations ($P_{uncorrected}$<0.05) between Horvath-EAA/Hannum-EAA and other health and behavioural**
343 **traits.**
344

Phenotype	Trait	Genetic Correlation	SE	*P*-value
Horvath-EAA	Fathers age at death	-0.472	0.144	0.001
	Urate	0.278	0.089	0.002
	Waist-to-hip ratio	0.194	0.064	0.002
	Waist circumference	0.178	0.064	0.005
	ICV	-0.403	0.163	0.013
	Forced expiratory volume in 1 second (FEV1)/Forced Vital capacity(FVC)	-0.170	0.078	0.030
	Extreme waist-to-hip ratio	0.306	0.146	0.036
	Child birth weight	-0.274	0.131	0.037
	Childhood IQ	-0.317	0.152	0.037
	Leucine	0.450	0.222	0.043
	Glycoprotein acetyls; mainly a1-acid glycoprotein	0.360	0.183	0.049
Hannum-EAA	Waist-to-hip ratio	0.225	0.062	0.0003
	Waist circumference	0.210	0.067	0.002
	Parents age at death	-0.455	0.148	0.002
	Type 2 Diabetes	0.331	0.114	0.004
	Years of schooling 2013	-0.231	0.083	0.005
	Years of schooling 2016	-0.162	0.058	0.006
	Birth weight	0.211	0.079	0.007
	HDL cholesterol	-0.210	0.082	0.010
	Former vs Current smoker	-0.330	0.130	0.011
	Forced expiratory volume in 1 second (FEV1)	-0.239	0.095	0.012
	Forced expiratory volume in 1 second (FEV1)	-0.371	0.149	0.013
	Hip circumference	0.163	0.066	0.013
	Intelligence	-0.169	0.070	0.016
	Cigarettes smoked per day	0.326	0.138	0.018
	Ever vs never smoked	0.202	0.088	0.022
	College completion	-0.195	0.086	0.023

	Age of first birth	-0.156	0.070	0.026
	HOMA-B	0.305	0.137	0.026
	Fasting insulin main effect	0.237	0.107	0.027
	HbA1C	-0.277	0.126	0.028
	Childhood IQ	-0.286	0.130	0.028
	Fathers age at death	-0.287	0.131	0.028
	Triglycerides	0.136	0.065	0.036
	Phospholipids in medium LDL	-0.410	0.200	0.040
	Free cholesterol in large LDL	-0.485	0.237	0.041
	Anorexia Nervosa	-0.152	0.074	0.041
	Amyotrophic lateral sclerosis	0.363	0.178	0.042
	Obesity class 1	0.135	0.067	0.042
	Years of schooling (proxy cognitive performance)	-0.171	0.084	0.042
	Phospholipids in large LDL	-0.471	0.232	0.043
	Phospholipids in very small VLDL	-0.373	0.184	0.043
	Free cholesterol in IDL	-0.439	0.220	0.046
	Celiac disease	-0.265	0.134	0.047
	Extreme waist-to-hip ratio	0.285	0.145	0.048
	Total cholesterol in large LDL	-0.430	0.219	0.049

Genetic correlations were determined using bivariate Linkage Disequilibrium score regression implemented in the online software LD Hub. SE is the standard error of the genetic correlation estimate; *P*-value is the association *P*-value for the genetic correlation estimate; ICV – intracranial volume; LDL – low density lipoprotein; IDL – intermediate density lipoprotein; VLDL – very low density lipoprotein.

Both epigenetic age acceleration measures had nominally significant positive genetic correlations with a range of traits pertaining to adiposity, and negative correlations with father's age at death and childhood IQ. Nominally significant genetic correlations were observed between Hannum-EAA, but not Horvath-EAA, and a wide range of traits including measures relating to education, smoking behaviour, various lipid- and cholesterol-related measures, diabetes and related glycemic measures, and parent's age at death. Some of these results have previously been reported (19), but many are novel. The current study did, however, fail to replicate a number of previously reported correlations, including with age at menopause (19). Details of the genetic correlations of all the tested traits with Horvath-EAA and Hannum-EAA are given in **Tables V and W in S1 Data**, respectively.

Discussion

This study investigated genetic markers of epigenetic ageing in a sample of 13,493 individuals of European ancestry. We examined genetic determinants of both Horvath-based (adjusted for the composition of age-related blood cells) and Hannum-based (immune system-associated) epigenetic age acceleration, sometimes referred to as 'intrinsic' and 'extrinsic' epigenetic age acceleration, to gain insight into the regulation of epigenetic ageing. We report several novel findings in addition to replicating a sub-set of previous results. The meta-analysis of Horvath-EAA identified ten independent associated SNPs, doubling the number reported to date, and highlighted 21 genes involved in Horvath-based epigenetic ageing. A single genome-wide significant variant was identified for Hannum-EAA, along with 12 implicated genes. We uncovered limited evidence of functionality within some associated genomic loci, with many SNPs located in regions of open chromatin and a smaller number in regulatory regions. Some loci also contained regions where genetic variation is predicted to be deleterious.

A number of the genes significantly associated with Horvath-EAA are related to metabolism (*NHLRC1*, *TPMT*, *KDM1B*, and *ESYT3*), consistent with several studies reporting phenotypic associations between Horvath-based EAA and metabolic syndrome characteristics and supporting the suggestion of a role in tracking metabolic ageing (14,18). Others are involved in immune system pathways (*TRIM59*, *KPNA4*, *EDARADD*), while several have roles in cellular processes linked to ageing: apoptosis and autophagy (*FAIM*), ageing and autophagy (*TERT*), and coordinating vital cell functions (*PIK3CB*). *PIK3CB* plays a role in the signal transduction of insulin and insulin-like pathways (42), and genetic variants at this locus have been related to insulin-like growth factor levels in plasma, and human longevity (43).

Genes associated with Hannum-based EAA, often referred to as immune system ageing, include several involved in innate immune system pathways (e.g. *TRIM46* and *MUC1*) or with metabolic and immune system functions (*MANBA*, *UBE2D3*). Other associated genes of interest include those with roles relating to ageing and longevity: *MTRNR2L7* is a neuroprotective and anti-apoptotic factor, and *CISD2* regulates autophagy and is a fundamentally important regulator of lifespan. Mouse studies indicate that *CISD2* ameliorates age-associated degeneration of skin, skeletal muscle, and neurons, protects mitochondria from age-related damage and functional decline, and attenuates age-associated reduction in energy metabolism (44), while *CISD2* deficiency leads to a number of phenotypic features suggestive of premature ageing (45).

Our LD score regression analysis replicated the positive genetic correlations with central adiposity reported by Lu et al. (2018) at nominal significance levels, supporting the suggestion that observed phenotypic associations (14,18) may result in part from a shared genetic aetiology. We did not, however, replicate previously reported correlations between Horvath-EAA and metabolic disease-related traits or diabetes, and found these traits to be correlated with Hannum-EAA at only nominal significance levels in our larger sample (19). We also found no correlation between epigenetic age

acceleration and age at menopause. Nominally significant genetic correlations between Hannum-based, but not Horvath-based, epigenetic age acceleration, and lifestyle factors such as smoking behaviour and education level, provide some evidence for a genetic basis underlying the phenotypic results we reported previously (18), and provide tentative support to the hypothesis that Hannum-based epigenetic ageing is relatively sensitive to changes in environment and lifestyle. Father's age at death, a rough proxy for lifespan (46), was nominally significantly correlated with both EAA measures, and parents' age at death was additionally correlated with Hannum-EAA, consistent with a body of work demonstrating robustly that EAA predicts life span (10,11). Aside from these, genetic correlations with age-related traits were surprisingly few: it is possible that this could reflect an overly conservative correction for the multiple tests carried out, or low statistical power, rather than a genuine lack of correlations (**Table D in S1 Data**). While the mean χ^2 values (1.059 and 1.054 for Horvath-EAA and Hannum-EAA respectively) indicate a sufficient level of polygenicity within the dataset for use with LD score regression, the heritability Z-scores for Horvath-EAA and Hannum-EAA are 3.69 and 4.91 respectively. The recommendation is that genetic correlation analysis should be restricted to GWAS with a heritability Z-score of 4 or more, on the grounds of interpretability and power (41), so the Horvath-based results particularly should be interpreted with caution.

This study of epigenetic age acceleration benefits from having a large sample size. Increasing GWAS sample size increases the power to detect associated loci, and is often achieved, as in this case, by combining smaller studies in a meta-analysis. Meta-analytic GWAS are, however, sometimes hampered by differences in how a trait is measured between individual studies. In this instance, use of the online calculator to calculate the EAA measures and using the same algorithm and output columns for each study, mitigates this. The current study comprises only individuals of European ancestry, which confers a further advantage as epigenetic ageing rates have been shown

to differ between ethnicities (47). It should be noted, however, that although large for these phenotypes, the size of the sample studied here is still small in terms of GWASs of polygenic traits.

Despite the large sample overlap, some results of this study differ from those reported by Lu et al. (2018). One reason for this could be that only European-ancestry individuals were included in this analysis whereas the Lu study reports results from a mixed ancestry sample. Another likely contributing factor is the age ranges involved: the GS cohort, not included in Lu's analysis but which makes up 38% of the total sample in the current study, has a mean age of 48.5 years, 14.4 years younger than the mean age of the remaining cohorts. Given that epigenetic age changes over the life course, although not necessarily in parallel with chronological age, this could help explain the discrepancies between the studies.

Horvath-based and Hannum-based epigenetic age acceleration are thought to represent different aspects of ageing. Hannum-EAA has been described as a biomarker of immune system ageing, and has been found to be associated with a wide range of traits (14,18), indicating a sensitivity to variations in environment and lifestyle. By contrast, Horvath-EAA is considered to be a fundamental, intrinsic cellular ageing process, largely unrelated to lifestyle factors, although associations with a range of metabolic syndrome characteristics suggest a role in tracking metabolic ageing processes. Our results reflect this to a large degree, with more nominally significant genetic correlations found with Hannum-EAA than Horvath-EAA, including items relating to education, smoking, intelligence, and various cholesterol measures. Meanwhile the greater number of significant variants, genomic loci, and genes associated with Horvath-EAA are consistent with the hypothesis that this measure of 'cell-intrinsic' ageing is less related to lifestyle and more under genetic control, and thus more likely to remain relatively stable. Despite these differences, however, our results indicate some common features. The significant genetic correlation of 0.57 between the two measures suggests a moderate overlap in the genetic factors influencing the two phenotypes

453 despite the biomarkers being based on almost entirely distinct CpG sets. Both also appear to be
454 influenced by genes associated with metabolic and immune system pathways, although the specific
455 genes involved are different.
456
457 **Conclusions**
458 This study provided insight into the genetic determinants of differential biological ageing through
459 the identification of genes and genetic variants associated with epigenetic age acceleration. We
460 doubled the number of SNPs associated with Horvath-EAA reported to date, and report 21 genes
461 significantly associated with this phenotype, including *PIK3CB*, linked to human longevity. We
462 identified 12 Hannum-EAA-associated genes, one of which, *CISD2*, has a fundamental role in
463 lifespan control. Our results also highlighted differences in the genetic architecture of the Horvath-
464 based and Hannum-based EAA measures, with no genome-wide significant SNPs or genes common
465 to the two, providing substantial support for the hypothesis that they represent different aspects of
466 ageing.
467
468 While the genetic information coded by our DNA sequence remains largely fixed throughout the
469 lifetime, the expression of our genes is primarily regulated by epigenetic factors, which change over
470 time. Epigenetic age increases with, but not in parallel with, chronological age; individual
471 differences in the rate of epigenetic ageing potentially explain why trajectories of ageing differ
472 between individuals. Understanding what causes these differences could potentially inform
473 therapeutic interventions to delay the onset of age-related decline and improve ageing outcomes.
474
475
476 # Methods
477
478 **Generation Scotland cohort**

We carried out genome-wide association analyses of Horvath-EAA and Hannum-EAA in a subset of individuals (n=5,100) from the Generation Scotland: Scottish Family Health Study (GS) for whom both genetic and DNA methylation data were available. GS is a family- and population-based cohort recruited via general medical practices across Scotland; the recruitment protocol and sample characteristics are described in detail elsewhere (48,49). In brief, the full cohort comprises 23,960 individuals aged between 18 and 98 years. Pedigree information was available for all participants, detailed socio-demographic and clinical data were collected, and biological samples were taken for genotyping.

DNA methylation and derivation of epigenetic age acceleration variables in GS

DNA methylation data were obtained from peripheral blood (n=5,091) or saliva (n=10) samples for 5,101 individuals from GS, with quality control checks carried out using standard methods outlined in **S1 Text**, and described in full elsewhere (18). After QC, the dataset comprised beta-values for 860,928 methylation loci. Methylation-based age estimates (DNAm age) and epigenetic age acceleration variables (Horvath-EAA and Hannum-EAA, described in **S1 Text**) were obtained from the online DNA Methylation Age Calculator (https://dnamage.genetics.ucla.edu/) developed by Horvath (8). Normalised DNA methylation beta-values were submitted to the calculator, using the 'Advanced Analysis for Blood Data' option, and undergoing further normalisation within the calculator algorithm to make the data comparable to the training data of the epigenetic clock. One individual was flagged by the calculator as having a gender mismatch, and was therefore omitted from downstream analysis, leaving a total of 5,100 individuals for the GWAS of Horvath-EAA and Hannum-EAA in GS. Blood cell abundance measures were also estimated by the online calculator, based on DNA methylation levels, as described previously (50).

Genotyping, imputation, and quality control in GS

An overview of biological sample collection, DNA extraction, genotyping, imputation using the Haplotype Research Consortium reference panel (v1.1), and quality control for GS is included in **S1 Text**; full details have been described previously (51). A total of 20,032 individuals passed all quality control thresholds. Following the removal of monomorphic or multiallelic variants and SNPs with a low imputation quality or a minor allele frequency below 1%, an imputed dataset with 8,633,288 hard called variants remained to be used in the genome-wide association analysis.

GWAS of Horvath-EAA and Hannum-EAA in GS

GWAS of Horvath-EAA and Hannum-EAA in GS were conducted using mixed linear model based association (MLMA) analysis (52), implemented in GCTA (v1.25) (53), and adjusting for sex to account for the higher epigenetic age acceleration in men than in women (7,11,47). In order to account for population stratification, it is common to conduct ancestry-informative principal components analysis on the population in question, and use a number of the top-ranking PCs from this analysis as covariates in the GWAS. However, as GS is a family-based sample, we employed a different approach to capture population structure. In place of PCs, two genomic relationship matrices (GRMs) were included in the GWAS, as this method has been shown to account for potential upward biases due to excessive relationships, and thus allows the inclusion of closely and distantly related individuals in genetic analyses (54). The first GRM included pairwise relationship coefficients for all individuals, while the second had off-diagonal elements <0.05 set to 0; full details of the methods involved and construction of the GRMs is given elsewhere (55). The results of univariate LD score regression analysis (56) (**Table D in S1 Data**) indicate that the two GRMs adequately accounted for population stratification, so it was not necessary to include ancestry-informative PCs in the GWAS.

GWAS meta-analysis of Horvath-EAA and Hannum-EAA

We obtained summary statistics from the largest European-ancestry analysis of epigenetic age acceleration to date (n=8,393, Lu et al., 2018, summary information in **Table X in S1 Data**), and meta-analysed these with GS (details above). We chose not to include available data from non-European samples, despite the advantages of increased sample size, as different ethnicities have been shown to have different epigenetic ageing rates (47). Association summary statistics from the GWAS of the two EAA phenotypes in GS and the Lu et al. study were meta-analysed using the inverse variance-weighted approach, which weights effect sizes by sampling distribution. This analysis was implemented in METAL (57), conditional on each variant being available in both samples. As SNPs which co-located with CpGs from the Hannum- or Horvath-based DNAm age predictors had already been excluded from Lu et al.'s analysis, it was not necessary to repeat this step. This resulted in 5,932,107 genetic variants for Horvath-EAA and 5,931,171 variants for Hannum-EAA, in a meta-analysis dataset containing 13,493 participants.

The meta-analytic summary statistics produced by METAL were uploaded to FUMA (fuma.ctglab.nl) (58), which identified index SNPs and genomic risk loci related to epigenetic age acceleration. FUMA selects independent significant SNPs based on their having a genome-wide significant *P*-value ($P<5x10^{-8}$) and being independent from each other ($r^2<0.6$ by default) within a 250kb window. The European subset of the 1000 Genomes phase 3 reference panel (59) was used to map LD. SNPs in LD with these independent significant SNPs ($r^2\geq0.6$) within a 250kb window, and which have a minor allele frequency (MAF)>1% within the 1000 Genomes reference panel, were included for further annotation and used for gene prioritization. A subset of the independent significant SNPs, those in LD with each other at $r^2<0.1$ within a 250kb window, were identified as lead SNPs. Genomic risk loci, including all independent signals that were physically close or overlapping in a single locus, were identified by merging any lead SNPs that were closer than 250kb apart (meaning that a genomic risk locus could contain multiple lead SNPs, with each locus represented by the lead SNP with the lowest *P*-value in that locus).

Conditional analysis was implemented using GCTA software (53) to ascertain whether associated genetic loci harboured more than one independent causal variant, conditioning on the lead SNP at the locus and using GS as the reference panel for inferring the LD pattern. SNPs which remained significantly associated ($P<5x10^{-8}$) with the phenotype after conditioning on the lead SNP were considered to be further independent associated variants.

Manhattan plots and quantile-quantile plots were generated in R version 3.2.3 using the 'qqman' package, and regional SNP association results were visualised with LocusZoom (60). SNPs which surpassed the threshold for genome-wide significance in our meta-analyses were checked against the NHGRI-EBI catalog of published GWAS (61,62) (www.ebi.ac.uk/gwas/) to determine whether they had previously been observed in association analysis.

Heritability analysis

To estimate the SNP-based heritability for Horvath-EAA and Hannum-EAA, univariate Linkage Disequilibrium score regression (56) was applied to the GWAS summary statistics for both measures. This method also provides metrics to evaluate the proportion of inflation in the test statistics caused by confounding biases such as residual population stratification, relative to genuine polygenicity. We used pre-computed LD scores, estimated from the European-ancestry samples in the 1000 Genomes Project (63).

SNP functional annotation

Functional annotation, using all SNPs located within the genomic risk loci which were nominally significant ($P<0.05$), had a MAF≥1%, and were in LD of $r^2\geq0.6$, was carried out in FUMA v1.3.0 (58). In order to investigate the functional consequences of variation at these SNPs, they were first

matched (based on chromosome, base pair position, reference and non-reference alleles) to a database containing functional annotations from a number of repositories:

- ANNOVAR categories (64), used to identify a SNP's function and determine its position within the genome.
- Combined Annotation Dependent Depletion (CADD) scores (21), a measure of the deleteriousness of genetic variation at a SNP to protein structure and function, with higher scores indicating more deleterious variants.
- RegulomeDB (RDB) scores (65), based on data from expression quantitative trait loci (eQTLs) as well as chromatin marks, with lower scores given to variants with the greatest evidence for having regulatory function.
- Chromatin states (66–68), indicating the level of accessibility of genomic regions, described on a 15 point scale, where lower chromatin scores indicate a greater level of accessibility to the genome at that site; generally, between 1 and 7 is considered an open chromatin state.

Gene-based analysis

Gene-based analysis was performed for each phenotype using the results of our association analysis, using default settings in MAGMA (Multi-marker Analysis of GenoMic Annotation) v1.6 (69), integrated within the FUMA web application. Summary statistics of SNPs located within protein-coding genes were aggregated to assess the simultaneous effect of all SNPs in the gene on the phenotype. The European panel of the 1000 Genomes phase 3 data was used as a reference panel to account for LD (59). Genetic variants were assigned to protein-coding genes obtained from Ensembl build 85, resulting in 17,798 genes being analysed. After Bonferroni correction (α=0.05/17,798), a threshold for genome-wide significant genes was defined at $P<2.809\times10^{-6}$.

Tissue Expression analysis

To determine whether differential expression levels of a gene in specific tissues relate to the

association of that gene with EAA, gene-property analysis was conducted using MAGMA, integrated within the FUMA web application, using average expression of genes per tissue type as a gene covariate. Four types of tissue expression analysis were performed separately, for 30 general tissue types, 53 specific tissue types (both taken from the GTEx v7 RNA-seq database (70,71)), 29 different ages of brain samples, and 11 developmental stages of brain samples (from BrainSpan (72)) , with Bonferroni correction over 30, 53, 29 and 11 tests respectively to control for multiple testing.

eQTL analysis

The independent genome-wide significant variants identified for Horvath-EAA and Hannum-EAA in the GWAS meta-analysis were assessed to determine whether they were potential expression quantitative trait loci (eQTLs), using the Genotype Tissue Expression Portal (GTEx) v7 (71), which used gene expression data from multiple human tissues linked to genotype data to provide information on eQTLs. eQTL mapping carried out within FUMA maps SNPs to genes which likely affect expression of those genes within 1Mb, i.e. *cis*-eQTLs.

Gene-set analysis

To assess whether the Horvath-EAA and Hannum-EAA GWAS meta-analysis results are enriched for various gene-sets and provide insight into the involvement of specific biological pathways in the genetic etiology of the phenotype, the gene-based analysis results were used to perform competitive gene-set and pathway analysis using default parameters in MAGMA v1.6, integrated within FUMA. The reference genome was 1000 genomes phase 3. This analysis used gene annotation files from the Molecular Signatures Database v5.2 for "Curated gene sets", covering chemical and genetic perturbations, and Canonical pathways, and "GO terms", covering three ontologies: biological process, cellular components, and molecular function. A total of 10,894 gene-sets were examined for enrichment in Horvath-EAA and Hannum-EAA, with a Bonferroni correction applied to control

for multiple testing. Thus genome-wide significance was defined at P=0.05/10,894=4.59x10^{-6}.

Genetic correlations

Cross trait LD score regression (73) was used to calculate genetic correlations between Horvath-based and Hannum-based EAA in our meta-analysis, and then between Horvath-EAA/Hannum-EAA and 218 other behavioural and disease-related traits for which GWAS summary data were available through LD Hub (41); traits derived from non-Caucasian or mixed ethnicity samples were removed prior to analysis. This method exploits the correlational structure of SNPs across the genome and uses test statistics provided from GWAS summary estimates to calculate the genetic correlations between traits (73). We checked whether our meta-analysis datasets had sufficient evidence of a polygenic signal, indicated by a heritability Z-score of >4 and a mean $\chi 2$ statistic of >1.02 (73). By default, a MAF filter of >1% was applied, and indels and strand ambiguous SNPs were removed. We filtered to HapMap3 SNPs, and SNPs whose alleles did not match those in the 1000 Genomes European reference sample were removed. LD scores and weights for use with European populations were downloaded from (http://www.broadinstitute.org/~bulik/eur_ldscores/). We did not constrain the intercepts in our analysis, as we could not quantify the exact amount of sample overlap between cohorts. False discovery rate correction was applied across the 218 traits to correct for multiple testing (74).

Ethics Statement

Generation Scotland received ethical approval from the NHS Tayside Committee on Medical Research Ethics (REC Reference Number: 05/S1401/89). GS has also been granted Research Tissue Bank status by the Tayside Committee on Medical Research Ethics (REC Reference Number: 10/S1402/20), providing generic ethical approval for a wide range of uses within medical research. All participants provided written informed consent. Details of ethics approval and consent to participate for the cohorts included in the Lu et al. (2018) study can be found in their publication.

Acknowledgements

We are grateful to the families and individuals who took part in all the cohort studies included in this meta-analysis: the Framington Heart Study, TwinsUK, Women's Health Initiate, European Prospective Investigation into Cancer–Norfolk, Baltimore Longitudinal Study of Aging, Invecchiare in Chianti, aging in the Chianti Area Study, Brisbane Systems Genetics Study, Lothian Birth Cohorts of 1921 and 1936, and Generation Scotland. We further acknowledge all those involved in participant recruitment, data collection, sample processing, and quality control procedures, including project managers, interviewers, clinical staff, laboratory technicians, clerical workers, research scientists, and statisticians.

684 **Fig 1. Manhattan plots for genome-wide meta-analyses (n=13,493) of Horvath-based and**
685 **Hannum-based epigenetic age acceleration.**

686 SNP-based Manhattan plots for Horvath-EAA and Hannum-EAA, with - $\log_{10}$ transformed *P*-values for each SNP
687 plotted against chromosomal location. The red line indicates the threshold for genome-wide significance ($P<5\times10^{-8}$)
688 and the blue line for suggestive associations ($P<1\times10^{-5}$).

689

690

691 **Fig 2. QQ plots for the meta-analyses of Horvath-based and Hannum-based epigenetic age**
692 **acceleration.**

693 Quantile-quantile plots for the genome-wide meta-analyses of Horvath-EAA and Hannum-EAA, showing the expected
694 distribution of GWAS test statistics, -log10(p), versus the observed distribution.

695

696

697

698

699

700

701

702

703

704

705

706

707

708

709

References

1. Niccoli T, Partridge L. Ageing as a Risk Factor for Disease. Curr Biol [Internet]. 2012 Sep 11 [cited 2018 Jun 4];22(17):R741–52. Available from: https://www.sciencedirect.com/science/article/pii/S0960982212008159?via%3Dihub

2. Rode L, Nordestgaard BG, Bojesen SE. Peripheral Blood Leukocyte Telomere Length and Mortality Among 64 637 Individuals From the General Population. JNCI J Natl Cancer Inst [Internet]. 2015 Jun 1 [cited 2018 Sep 25];107(6). Available from: https://academic.oup.com/jnci/article-lookup/doi/10.1093/jnci/djv074

3. Beck S, Rakyan VK. The methylome: approaches for global DNA methylation profiling. Trends Genet [Internet]. 2008 May 1 [cited 2018 May 14];24(5):231–7. Available from: https://www.sciencedirect.com/science/article/pii/S0168952508000577?via%3Dihub

4. Bollati V, Schwartz J, Wright R, Litonjua A, Tarantini L, Suh H, et al. Decline in genomic DNA methylation through aging in a cohort of elderly subjects. Mech Ageing Dev [Internet]. 2009 Apr [cited 2018 May 14];130(4):234–9. Available from: http://www.ncbi.nlm.nih.gov/pubmed/19150625

5. Christensen BC, Houseman EA, Marsit CJ, Zheng S, Wrensch MR, Wiemels JL, et al. Aging and Environmental Exposures Alter Tissue-Specific DNA Methylation Dependent upon CpG Island Context. Schübeler D, editor. PLoS Genet [Internet]. 2009 Aug 14 [cited 2018 May 14];5(8):e1000602. Available from: http://dx.plos.org/10.1371/journal.pgen.1000602

6. Shah S, McRae AF, Marioni RE, Harris SE, Gibson J, Henders AK, et al. Genetic and environmental exposures constrain epigenetic drift over the human life course. Genome Res [Internet]. 2014 Nov 1 [cited 2018 May 14];24(11):1725–33. Available from: http://www.ncbi.nlm.nih.gov/pubmed/25249537

7. Hannum G, Guinney J, Zhao L, Zhang L, Hughes G, Sadda S, et al. Genome-wide methylation profiles reveal quantitative views of human aging rates. Mol Cell [Internet]. 2013 Jan 24 [cited 2018 May 14];49(2):359–67. Available from: http://www.ncbi.nlm.nih.gov/pubmed/23177740

8. Horvath S. DNA methylation age of human tissues and cell types. Genome Biol [Internet]. 2013 Dec 10 [cited 2018 May 14];14(10):R115. Available from: http://genomebiology.biomedcentral.com/articles/10.1186/gb-2013-14-10-r115

9. Marioni RE, Shah S, McRae AF, Ritchie SJ, Muniz-Terrera G, Harris SE, et al. The epigenetic clock is correlated with physical and cognitive fitness in the Lothian Birth Cohort 1936. Int J Epidemiol [Internet]. 2015 Aug 1 [cited 2018 May 14];44(4):1388–96. Available from: https://academic.oup.com/ije/article-lookup/doi/10.1093/ije/dyu277

10. Chen BH, Marioni RE, Colicino E, Peters MJ, Ward-Caviness CK, Tsai P-C, et al. DNA methylation-based measures of biological age: meta-analysis predicting time to death. Aging (Albany NY) [Internet]. 2016 Sep 28 [cited 2018 May 14];8(9):1844–65. Available from: http://www.ncbi.nlm.nih.gov/pubmed/27690265

11. Marioni RE, Shah S, McRae AF, Chen BH, Colicino E, Harris SE, et al. DNA methylation age of blood predicts all-cause mortality in later life. Genome Biol [Internet]. 2015 Jan 30 [cited 2018 May 14];16(1):25. Available from: http://genomebiology.com/2015/16/1/25

12. Fagnoni FF, Vescovini R, Passeri G, Bologna G, Pedrazzoni M, Lavagetto G, et al. Shortage of circulating naive CD8(+) T cells provides new insights on immunodeficiency in aging. Blood [Internet]. 2000 May 1 [cited 2019 Jan 21];95(9):2860–8. Available from: http://www.ncbi.nlm.nih.gov/pubmed/10779432

13. Miller RA. The aging immune system: primer and prospectus. Science [Internet]. 1996 Jul 5 [cited 2019 Jan 21];273(5271):70–4. Available from: http://www.ncbi.nlm.nih.gov/pubmed/8658199

14. Quach A, Levine ME, Tanaka T, Lu AT, Chen BH, Ferrucci L, et al. Epigenetic clock analysis of diet, exercise, education, and lifestyle factors. Aging (Albany NY) [Internet]. 2017 Feb 14 [cited 2018 May 14];9(2):419–46. Available from: http://www.ncbi.nlm.nih.gov/pubmed/28198702

15. Levine ME, Lu AT, Bennett DA, Horvath S. Epigenetic age of the pre-frontal cortex is associated with neuritic plaques, amyloid load, and Alzheimer's disease related cognitive functioning. Aging (Albany NY) [Internet]. 2015 Dec [cited 2018 May 14];7(12):1198–211. Available from: http://www.ncbi.nlm.nih.gov/pubmed/26684672

16. Levine ME, Lu AT, Chen BH, Hernandez DG, Singleton AB, Ferrucci L, et al. Menopause accelerates biological aging. Proc Natl Acad Sci U S A [Internet]. 2016 Aug 16 [cited 2018 May 14];113(33):9327–32. Available from: http://www.ncbi.nlm.nih.gov/pubmed/27457926

17. Horvath S, Ritz BR. Increased epigenetic age and granulocyte counts in the blood of Parkinson's disease patients. Aging (Albany NY) [Internet]. 2015 Dec [cited 2018 May 14];7(12):1130–42. Available from: http://www.ncbi.nlm.nih.gov/pubmed/26655927

765 18. McCartney DL, Stevenson AJ, Walker RM, Gibson J, Morris SW, Campbell A, et al. DNA methylation age
766 acceleration and risk factors for Alzheimer's disease. bioRxiv [Internet]. 2018 Mar 8 [cited 2018 Jun
767 12];278945. Available from: https://www.biorxiv.org/content/early/2018/03/08/278945

768 19. Lu AT, Xue L, Salfati EL, Chen BH, Ferrucci L, Levy D, et al. GWAS of epigenetic aging rates in blood reveals a
769 critical role for TERT. Nat Commun [Internet]. 2018 Dec 26 [cited 2018 May 14];9(1):387. Available from:
770 http://www.nature.com/articles/s41467-017-02697-5

771 20. Twine NA, Harkness L, Kassem M, Wilkins MR. Transcription factor ZNF25 is associated with osteoblast
772 differentiation of human skeletal stem cells. BMC Genomics [Internet]. 2016 [cited 2018 Nov 5];17(1):872.
773 Available from: http://www.ncbi.nlm.nih.gov/pubmed/27814695

774 21. Kircher M, Witten DM, Jain P, O'Roak BJ, Cooper GM, Shendure J. A general framework for estimating the
775 relative pathogenicity of human genetic variants. Nat Genet [Internet]. 2014 Mar 2 [cited 2018 May
776 14];46(3):310–5. Available from: http://www.nature.com/articles/ng.2892

777 22. Saheki Y, Bian X, Schauder CM, Sawaki Y, Surma MA, Klose C, et al. Control of plasma membrane lipid
778 homeostasis by the extended synaptotagmins. Nat Cell Biol [Internet]. 2016 May 11 [cited 2018 Jun
779 11];18(5):504–15. Available from: http://www.nature.com/articles/ncb3339

780 23. Belinky F, Nativ N, Stelzer G, Zimmerman S, Iny Stein T, Safran M, et al. PathCards: multi-source consolidation
781 of human biological pathways. Database (Oxford) [Internet]. 2015 [cited 2018 Jun 12];2015. Available from:
782 http://www.ncbi.nlm.nih.gov/pubmed/25725062

783 24. Segura MF, Sole C, Pascual M, Moubarak RS, Jose Perez-Garcia M, Gozzelino R, et al. The Long Form of Fas
784 Apoptotic Inhibitory Molecule Is Expressed Specifically in Neurons and Protects Them against Death Receptor-
785 Triggered Apoptosis. J Neurosci [Internet]. 2007 Oct 17 [cited 2018 Jun 12];27(42):11228–41. Available from:
786 http://www.ncbi.nlm.nih.gov/pubmed/17942717

787 25. Krasilnikov MA. Phosphatidylinositol-3 kinase dependent pathways: the role in control of cell growth, survival,
788 and malignant transformation. Biochemistry (Mosc) [Internet]. 2000 Jan [cited 2018 Jun 12];65(1):59–67.
789 Available from: http://www.ncbi.nlm.nih.gov/pubmed/10702641

790 26. Castaing-Berthou A, Malet N, Radojkovic C, Cabou C, Gayral S, Martinez LO, et al. PI3Kβ Plays a Key Role in
791 Apolipoprotein A-I-Induced Endothelial Cell Proliferation Through Activation of the Ecto-F1-ATPase/P2Y1
792 Receptors. Cell Physiol Biochem [Internet]. 2017 [cited 2018 Jun 11];42(2):579–93. Available from:

http://www.ncbi.nlm.nih.gov/pubmed/28578353

27. Couarch P, Vernia S, Gourfinkel-An I, Lesca G, Gataullina S, Fedirko E, et al. Lafora progressive myoclonus epilepsy: NHLRC1 mutations affect glycogen metabolism. J Mol Med (Berl) [Internet]. 2011 Sep [cited 2018 Jun 11];89(9):915–25. Available from: http://www.ncbi.nlm.nih.gov/pubmed/21505799

28. Laity JH, Lee BM, Wright PE. Zinc finger proteins: new insights into structural and functional diversity. Curr Opin Struct Biol [Internet]. 2001 Feb 1 [cited 2018 Oct 4];11(1):39–46. Available from: https://www.sciencedirect.com/science/article/pii/S0959440X00001676?via%3Dihub

29. Krynetski EY, Evans WE. Genetic polymorphism of thiopurine S-methyltransferase: molecular mechanisms and clinical importance. Pharmacology [Internet]. 2000 Sep [cited 2018 Jun 11];61(3):136–46. Available from: http://www.ncbi.nlm.nih.gov/pubmed/10971199

30. Nagaoka K, Hino S, Sakamoto A, Anan K, Takase R, Umehara T, et al. Lysine-specific demethylase 2 suppresses lipid influx and metabolism in hepatic cells. Mol Cell Biol [Internet]. 2015 Apr [cited 2018 Jun 11];35(7):1068–80. Available from: http://www.ncbi.nlm.nih.gov/pubmed/25624347

31. Ozato K, Shin D-M, Chang T-H, Morse HC. TRIM family proteins and their emerging roles in innate immunity. Nat Rev Immunol [Internet]. 2008 Nov 1 [cited 2018 Jun 11];8(11):849–60. Available from: http://www.nature.com/articles/nri2413

32. Yang J, Lu C, Wei J, Guo Y, Liu W, Luo L, et al. Inhibition of KPNA4 attenuates prostate cancer metastasis. Oncogene [Internet]. 2017 [cited 2018 Jun 11];36(20):2868–78. Available from: http://www.ncbi.nlm.nih.gov/pubmed/27941876

33. Jakob S, Haendeler J. Molecular mechanisms involved in endothelial cell aging: role of telomerase reverse transcriptase. Z Gerontol Geriatr [Internet]. 2007 Oct [cited 2018 Jun 11];40(5):334–8. Available from: http://link.springer.com/10.1007/s00391-007-0482-y

34. Mattson MP, Klapper W. Emerging roles for telomerase in neuronal development and apoptosis. J Neurosci Res [Internet]. 2001 Jan 1 [cited 2018 Jun 11];63(1):1–9. Available from: http://doi.wiley.com/10.1002/1097-4547%2820010101%2963%3A1%3C1%3A%3AAID-JNR1%3E3.0.CO%3B2-I

35. Tajima H, Niikura T, Hashimoto Y, Ito Y, Kita Y, Terashita K, et al. Evidence for in vivo production of Humanin peptide, a neuroprotective factor against Alzheimer's disease-related insults. Neurosci Lett [Internet]. 2002

May 24 [cited 2018 Jun 11];324(3):227–31. Available from: https://www.sciencedirect.com/science/article/pii/S0304394002001994?via%3Dihub

36. Guo B, Zhai D, Cabezas E, Welsh K, Nouraini S, Satterthwait AC, et al. Humanin peptide suppresses apoptosis by interfering with Bax activation. Nature [Internet]. 2003 May 4 [cited 2018 Jun 11];423(6938):456–61. Available from: http://www.nature.com/articles/nature01627

37. Agrawal B, Krantz MJ, Parker J, Longenecker BM. Expression of MUC1 mucin on activated human T cells: implications for a role of MUC1 in normal immune regulation. Cancer Res [Internet]. 1998 Sep 15 [cited 2018 Jun 11];58(18):4079–81. Available from: http://www.ncbi.nlm.nih.gov/pubmed/9751614

38. Shi Y, Yuan B, Zhu W, Zhang R, Li L, Hao X, et al. Ube2D3 and Ube2N are essential for RIG-I-mediated MAVS aggregation in antiviral innate immunity. Nat Commun [Internet]. 2017 May 4 [cited 2018 Jun 12];8:15138. Available from: http://www.nature.com/doifinder/10.1038/ncomms15138

39. Chen Y-F, Wu C-Y, Kirby R, Kao C-H, Tsai T-F. A role for the CISD2 gene in lifespan control and human disease. Ann N Y Acad Sci [Internet]. 2010 Jul [cited 2018 Jun 12];1201(1):58–64. Available from: http://doi.wiley.com/10.1111/j.1749-6632.2010.05619.x

40. Wang C-H, Kao C-H, Chen Y-F, Wei Y-H, Tsai T-F. Cisd2 mediates lifespan: is there an interconnection among Ca $^{2+}$ homeostasis, autophagy, and lifespan? Free Radic Res [Internet]. 2014 Sep 29 [cited 2018 Jun 12];48(9):1109–14. Available from: http://www.tandfonline.com/doi/full/10.3109/10715762.2014.936431

41. Zheng J, Erzurumluoglu AM, Elsworth BL, Kemp JP, Howe L, Haycock PC, et al. LD Hub: a centralized database and web interface to perform LD score regression that maximizes the potential of summary level GWAS data for SNP heritability and genetic correlation analysis. Bioinformatics [Internet]. 2017 Jan 15 [cited 2018 May 15];33(2):272–9. Available from: https://academic.oup.com/bioinformatics/article-lookup/doi/10.1093/bioinformatics/btw613

42. Kops GJPL, Medema RH, Glassford J, Essers MAG, Dijkers PF, Coffer PJ, et al. Control of cell cycle exit and entry by protein kinase B-regulated forkhead transcription factors. Mol Cell Biol [Internet]. 2002 Apr [cited 2018 May 23];22(7):2025–36. Available from: http://www.ncbi.nlm.nih.gov/pubmed/11884591

43. Bonafè M, Barbieri M, Marchegiani F, Olivieri F, Ragno E, Giampieri C, et al. Polymorphic Variants of Insulin-Like Growth Factor I (IGF-I) Receptor and Phosphoinositide 3-Kinase Genes Affect IGF-I Plasma Levels and Human Longevity: Cues for an Evolutionarily Conserved Mechanism of Life Span Control. J Clin Endocrinol

Metab [Internet]. 2003 Jul 1 [cited 2018 May 23];88(7):3299–304. Available from: https://academic.oup.com/jcem/article-lookup/doi/10.1210/jc.2002-021810

44. Wu C-Y, Chen Y-F, Wang C-H, Kao C-H, Zhuang H-W, Chen C-C, et al. A persistent level of Cisd2 extends healthy lifespan and delays aging in mice. Hum Mol Genet [Internet]. 2012 Sep 15 [cited 2018 May 23];21(18):3956–68. Available from: https://academic.oup.com/hmg/article-lookup/doi/10.1093/hmg/dds210

45. Chen Y-F, Kao C-H, Chen Y-T, Wang C-H, Wu C-Y, Tsai C-Y, et al. Cisd2 deficiency drives premature aging and causes mitochondria-mediated defects in mice. Genes Dev [Internet]. 2009 May 15 [cited 2018 May 23];23(10):1183–94. Available from: http://www.ncbi.nlm.nih.gov/pubmed/19451219

46. Vågerö D, Aronsson V, Modin B. Why is parental lifespan linked to children's chances of reaching a high age? A transgenerational hypothesis. SSM - Popul Heal [Internet]. 2018 Apr [cited 2018 Nov 5];4:45–54. Available from: http://www.ncbi.nlm.nih.gov/pubmed/29349272

47. Horvath S, Gurven M, Levine ME, Trumble BC, Kaplan H, Allayee H, et al. An epigenetic clock analysis of race/ethnicity, sex, and coronary heart disease. Genome Biol [Internet]. 2016 Dec 11 [cited 2018 May 14];17(1):171. Available from: http://genomebiology.biomedcentral.com/articles/10.1186/s13059-016-1030-0

48. Smith BH, Campbell H, Blackwood D, Connell J, Connor M, Deary IJ, et al. Generation Scotland: the Scottish Family Health Study; a new resource for researching genes and heritability. BMC Med Genet [Internet]. 2006 Dec 2 [cited 2018 May 15];7(1):74. Available from: http://bmcmedgenet.biomedcentral.com/articles/10.1186/1471-2350-7-74

49. Smith BH, Campbell A, Linksted P, Fitzpatrick B, Jackson C, Kerr SM, et al. Cohort Profile: Generation Scotland: Scottish Family Health Study (GS:SFHS). The study, its participants and their potential for genetic research on health and illness. Int J Epidemiol [Internet]. 2013 Jun 1 [cited 2018 May 15];42(3):689–700. Available from: https://academic.oup.com/ije/article-lookup/doi/10.1093/ije/dys084

50. Houseman EA, Accomando WP, Koestler DC, Christensen BC, Marsit CJ, Nelson HH, et al. DNA methylation arrays as surrogate measures of cell mixture distribution. BMC Bioinformatics [Internet]. 2012 May 8 [cited 2018 Jun 4];13:86. Available from: http://www.ncbi.nlm.nih.gov/pubmed/22568884

51. Nagy R, Boutin TS, Marten J, Huffman JE, Kerr SM, Campbell A, et al. Exploration of haplotype research consortium imputation for genome-wide association studies in 20,032 Generation Scotland participants. Genome Med [Internet]. 2017 Dec 7 [cited 2018 May 15];9(1):23. Available from:

876 http://genomemedicine.biomedcentral.com/articles/10.1186/s13073-017-0414-4

877 52. Yang J, Zaitlen NA, Goddard ME, Visscher PM, Price AL. Advantages and pitfalls in the application of mixed-
878 model association methods. Nat Genet [Internet]. 2014 Feb 1 [cited 2018 May 14];46(2):100–6. Available
879 from: http://www.nature.com/articles/ng.2876

880 53. Yang J, Lee SH, Goddard ME, Visscher PM. GCTA: A Tool for Genome-wide Complex Trait Analysis. Am J Hum
881 Genet [Internet]. 2011 Jan 7 [cited 2018 May 14];88(1):76–82. Available from:
882 https://www.sciencedirect.com/science/article/pii/S0002929710005987?via%3Dihub

883 54. Zaitlen N, Kraft P, Patterson N, Pasaniuc B, Bhatia G, Pollack S, et al. Using Extended Genealogy to Estimate
884 Components of Heritability for 23 Quantitative and Dichotomous Traits. Visscher PM, editor. PLoS Genet
885 [Internet]. 2013 May 30 [cited 2018 May 15];9(5):e1003520. Available from:
886 http://dx.plos.org/10.1371/journal.pgen.1003520

887 55. Hall LS, Adams MJ, Arnau-Soler A, Clarke T-K, Howard DM, Zeng Y, et al. Genome-wide meta-analyses of
888 stratified depression in Generation Scotland and UK Biobank. Transl Psychiatry [Internet]. 2018 Dec; Available
889 from: https://doi.org/10.1038/s41398-017-0034-1

890 56. Bulik-Sullivan BK, Loh P-R, Finucane HK, Ripke S, Yang J, Patterson N, et al. LD Score regression distinguishes
891 confounding from polygenicity in genome-wide association studies. Nat Genet [Internet]. 2015 Feb 2 [cited
892 2018 May 14];47(3):291–5. Available from: http://www.nature.com/doifinder/10.1038/ng.3211

893 57. Willer CJ, Li Y, Abecasis GR. METAL: fast and efficient meta-analysis of genomewide association scans.
894 Bioinformatics [Internet]. 2010 Sep 1 [cited 2018 May 14];26(17):2190–1. Available from:
895 http://www.ncbi.nlm.nih.gov/pubmed/20616382

896 58. Watanabe K, Taskesen E, van Bochoven A, Posthuma D. Functional mapping and annotation of genetic
897 associations with FUMA. Nat Commun [Internet]. 2017 Dec 28 [cited 2018 May 14];8(1):1826. Available from:
898 http://www.nature.com/articles/s41467-017-01261-5

899 59. Gibbs RA, Boerwinkle E, Doddapaneni H, Han Y, Korchina V, Kovar C, et al. A global reference for human
900 genetic variation. Nature [Internet]. 2015 Oct 1 [cited 2018 Sep 28];526(7571):68–74. Available from:
901 http://www.nature.com/articles/nature15393

902 60. Pruim RJ, Welch RP, Sanna S, Teslovich TM, Chines PS, Gliedt TP, et al. LocusZoom: regional visualization of

genome-wide association scan results. Bioinformatics [Internet]. 2010 Sep 15 [cited 2018 May 15];26(18):2336–7. Available from: https://academic.oup.com/bioinformatics/article-lookup/doi/10.1093/bioinformatics/btq419

61. Welter D, MacArthur J, Morales J, Burdett T, Hall P, Junkins H, et al. The NHGRI GWAS Catalog, a curated resource of SNP-trait associations. Nucleic Acids Res [Internet]. 2014 Jan 1 [cited 2018 May 15];42(D1):D1001–6. Available from: https://academic.oup.com/nar/article-lookup/doi/10.1093/nar/gkt1229

62. MacArthur J, Bowler E, Cerezo M, Gil L, Hall P, Hastings E, et al. The new NHGRI-EBI Catalog of published genome-wide association studies (GWAS Catalog). Nucleic Acids Res [Internet]. 2017 Jan 4 [cited 2018 May 15];45(D1):D896–901. Available from: https://academic.oup.com/nar/article-lookup/doi/10.1093/nar/gkw1133

63. Consortium T 1000 GP. An integrated map of genetic variation from 1,092 human genomes. Nature [Internet]. 2012 Nov [cited 2018 May 14];491(7422):56–65. Available from: http://www.nature.com/articles/nature11632

64. Wang K, Li M, Hakonarson H. ANNOVAR: functional annotation of genetic variants from high-throughput sequencing data. Nucleic Acids Res [Internet]. 2010 Sep 1 [cited 2018 May 14];38(16):e164–e164. Available from: https://academic.oup.com/nar/article-lookup/doi/10.1093/nar/gkq603

65. Boyle AP, Hong EL, Hariharan M, Cheng Y, Schaub MA, Kasowski M, et al. Annotation of functional variation in personal genomes using RegulomeDB. Genome Res [Internet]. 2012 Sep [cited 2018 May 14];22(9):1790–7. Available from: http://www.ncbi.nlm.nih.gov/pubmed/22955989

66. Ernst J, Kellis M. ChromHMM: automating chromatin-state discovery and characterization. Nat Methods [Internet]. 2012 Mar 1 [cited 2018 May 14];9(3):215–6. Available from: http://www.nature.com/articles/nmeth.1906

67. Kundaje A, Meuleman W, Ernst J, Bilenky M, Yen A, Heravi-Moussavi A, et al. Integrative analysis of 111 reference human epigenomes. Nature [Internet]. 2015 Feb 19 [cited 2018 May 14];518(7539):317–30. Available from: http://www.nature.com/articles/nature14248

68. Zhu Z, Zhang F, Hu H, Bakshi A, Robinson MR, Powell JE, et al. Integration of summary data from GWAS and eQTL studies predicts complex trait gene targets. Nat Genet [Internet]. 2016 May 28 [cited 2018 May 14];48(5):481–7. Available from: http://www.nature.com/articles/ng.3538

69. de Leeuw CA, Mooij JM, Heskes T, Posthuma D. MAGMA: generalized gene-set analysis of GWAS data. PLoS Comput Biol [Internet]. 2015 Apr [cited 2018 May 15];11(4):e1004219. Available from: http://www.ncbi.nlm.nih.gov/pubmed/25885710

70. GTEx Consortium Gte. Human genomics. The Genotype-Tissue Expression (GTEx) pilot analysis: multitissue gene regulation in humans. Science [Internet]. 2015 May 8 [cited 2018 May 15];348(6235):648–60. Available from: http://www.ncbi.nlm.nih.gov/pubmed/25954001

71. Aguet F, Brown AA, Castel SE, Davis JR, He Y, Jo B, et al. Genetic effects on gene expression across human tissues. Nature [Internet]. 2017 Oct 11 [cited 2018 May 15];550(7675):204–13. Available from: http://www.nature.com/doifinder/10.1038/nature24277

72. Miller JA, Ding S-L, Sunkin SM, Smith KA, Ng L, Szafer A, et al. Transcriptional landscape of the prenatal human brain. Nature [Internet]. 2014 Apr 2 [cited 2018 May 15];508(7495):199–206. Available from: http://www.nature.com/doifinder/10.1038/nature13185

73. Bulik-Sullivan B, Finucane HK, Anttila V, Gusev A, Day FR, Loh P-R, et al. An atlas of genetic correlations across human diseases and traits. Nat Genet [Internet]. 2015 Nov 28 [cited 2018 May 15];47(11):1236–41. Available from: http://www.nature.com/articles/ng.3406

74. Benjamini Y, Hochberg Y. Controlling the False Discovery Rate: A Practical and Powerful Approach to Multiple Testing. Source J R Stat Soc Ser B [Internet]. 1995 [cited 2018 May 15];57(1):289–300. Available from: http://www.jstor.org/stable/2346101

Supporting Information

S1 Text: Supplementary Information

S1 Text contains further information on the Hannum and Horvath epigenetic clocks, measures of epigenetic age and epigenetic age acceleration, DNA methylation in GS, derivation of epigenetic age and epigenetic age acceleration variables in GS, genotyping, imputation, and quality control in GS.

S1 Data: Supplementary Tables

Table A: Summary of age and estimated epigenetic age variables in Generation Scotland

Table B: Independent variants with a genome-wide significant association ($P<5x10^{-8}$) with epigenetic age acceleration in the Generation Scotland cohort

Table C: Independent variants with a *P*-value $<5x10^{-8}$ for association with Horvath-EAA/Hannum-EAA in the Lu et al. sample, and their corresponding effect size and significance in the Generation Scotland cohort

Table D: Estimated polygenicity and SNP-based heritability using LD score regression

Table E: Full details of independent variants with a genome-wide significant association ($P<5x10^{-8}$) with Horvath-based or Hannum-based epigenetic age acceleration

Table F: Independent variants with a *P*-value $<5x10^{-8}$ for association with Horvath-EAA/Hannum-EAA in the meta-analysis, and their corresponding effect size and significance in the Generation Scotland and Lu samples

Table G: Summary of the independent variants significantly associated with either Horvath-EAA or Hannum-EAA, and their association with both epigenetic age acceleration measures

Table H: Functional annotation of all SNPs in LD ($r^2 >= 0.6$) with FUMA-identified independent significant SNPs for Horvath-EAA

Table I: Functional annotation of all SNPs in LD (r^2 >= 0.6) with FUMA-identified independent significant SNPs for Hannum-EAA

Table J: MAGMA gene property analysis (30 general tissue types) for the meta-analysis of Horvath-EAA

Table K: MAGMA gene property analysis (53 specific tissue types) for the meta-analysis of Horvath-EAA

Table L: MAGMA gene property analysis (29 different ages of brain samples) for the meta-analysis of Horvath-EAA

Table M: MAGMA gene property analysis (11 different developmental stages of brain samples) for the meta-analysis of Horvath-EAA

Table N: MAGMA gene property analysis (30 general tissue types) for the meta-analysis of Hannum-EAA

Table O: MAGMA gene property analysis (53 specific tissue types) for the meta-analysis of Hannum-EAA

Table P: MAGMA gene property analysis (29 different ages of brain samples) for the meta-analysis of Hannum-EAA

Table Q: MAGMA gene property analysis (11 different developmental stages of brain samples) for the meta-analysis of Hannum-EAA

Table R: Expression quantitative trait loci identified by analysis of independent significant variants for Horvath-EAA and Hannum-EAA and the significance of their expression in the specified tissues

Table S: Genome-wide significant gene-based results ($P<2.809\text{x}10^{-6}$) obtained by MAGMA gene-based association analyses of Horvath-EAA and Hannum-EAA

Table T: Most associated gene sets for the GWAS meta-analysis of Horvath-EAA

Table U: Most associated gene sets for the GWAS meta-analysis of Hannum-EAA

Table V: Genetic correlations between Horvath-EAA and 218 other health and behavioural traits

Table W: Genetic correlations between Hannum-EAA and 218 other health and behavioural traits

Table X: Overview of study datasets

S2 Text: Supplementary Figures

Fig A: SNP-based Manhattan plot for the GWAS analysis of Horvath-based epigenetic age acceleration and Hannum-based epigenetic age acceleration in the GS cohort

Fig B: QQ plots for the GWAS of Horvath-EAA and Hannum-EAA in GS

Figs C-L: Regional association plots for the independent SNPs that are significantly associated with Horvath-EAA

Fig M: Regional association plot for the independent significantly associated SNP with Hannum-EAA

Fig N: Scatter plot of -log10(association *P*-value) for SNP-based GWAS of Horvath-EAA vs -log10(association *P*-value) for SNP-based GWAS of Hannum-EAA

Fig O: Scatter plot of -log10(association *P*-value) for gene-based GWAS of Horvath-EAA vs -log10(association *P*-value) for gene-based GWAS of Hannum-EAA

Fig P: Manhattan plots for the MAGMA gene-based association analysis for the GWAS meta-analysis of Horvath-based epigenetic age acceleration and Hannum-based epigenetic age acceleration

Fig Q: QQ plots for the gene-based association analyses of Horvath-EAA and Hannum-EAA

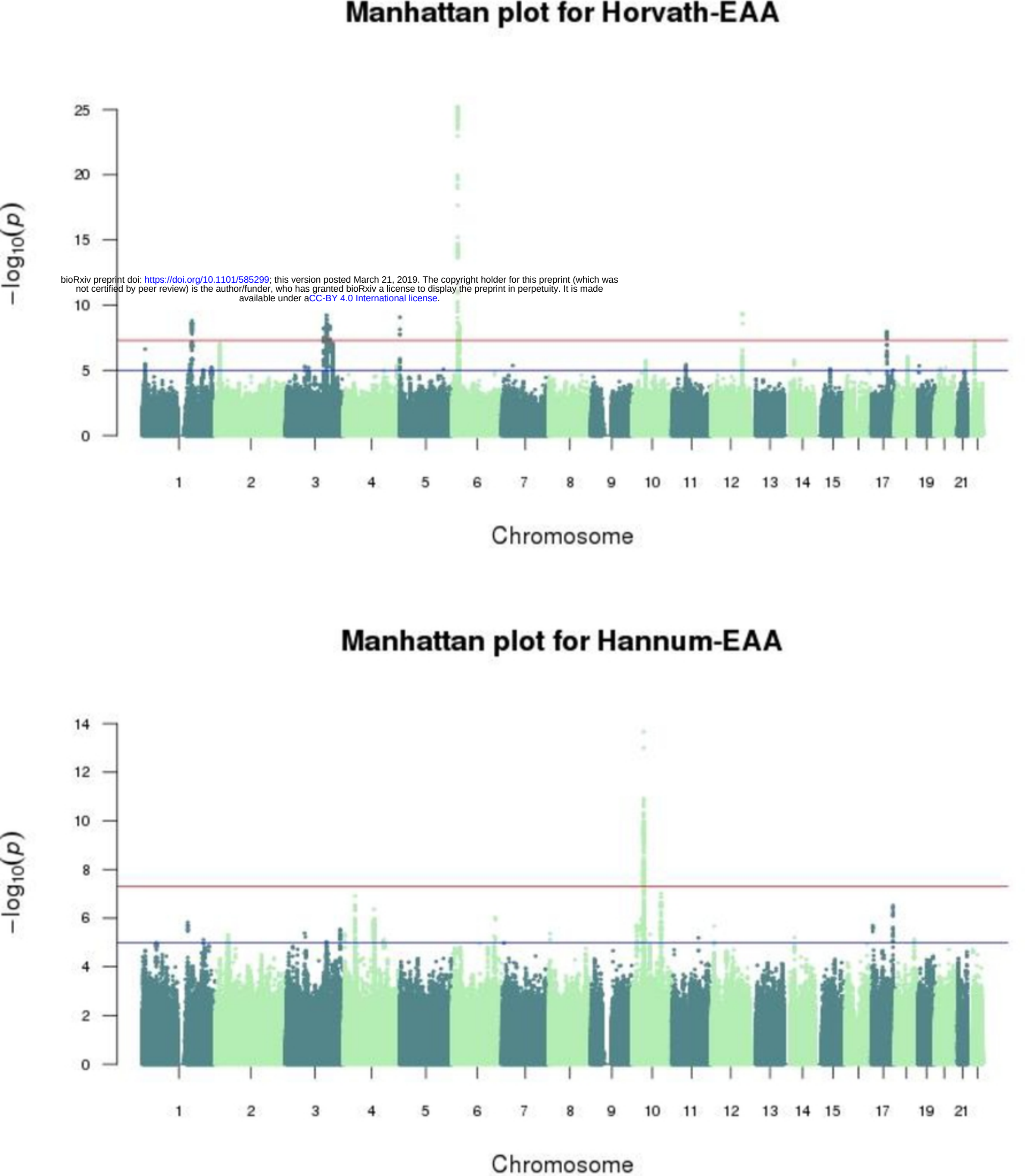

Figure 1

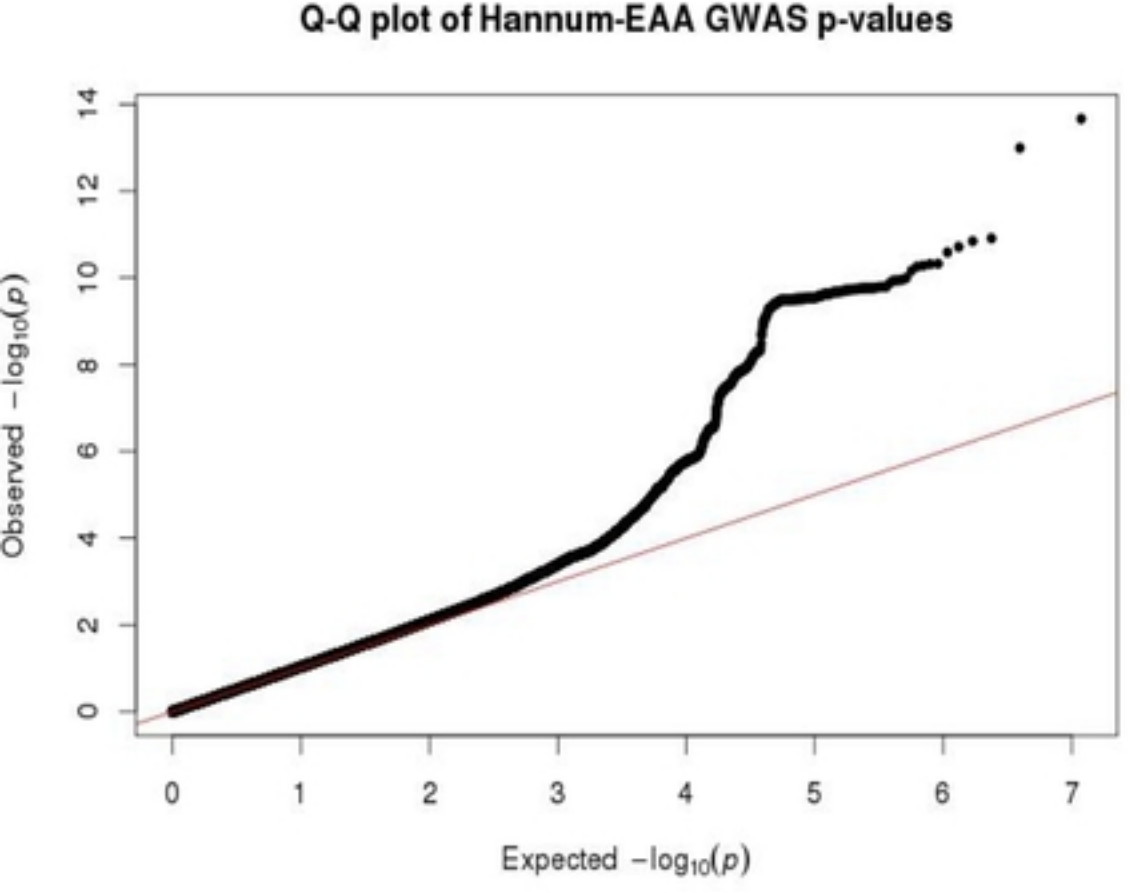
Q-Q plot of Hannum-EAA GWAS p-values
Observed $-\log_{10}(p)$
Expected $-\log_{10}(p)$
0
2
4
6
8
10
12
14
0
1
2
3
4
5
6
7

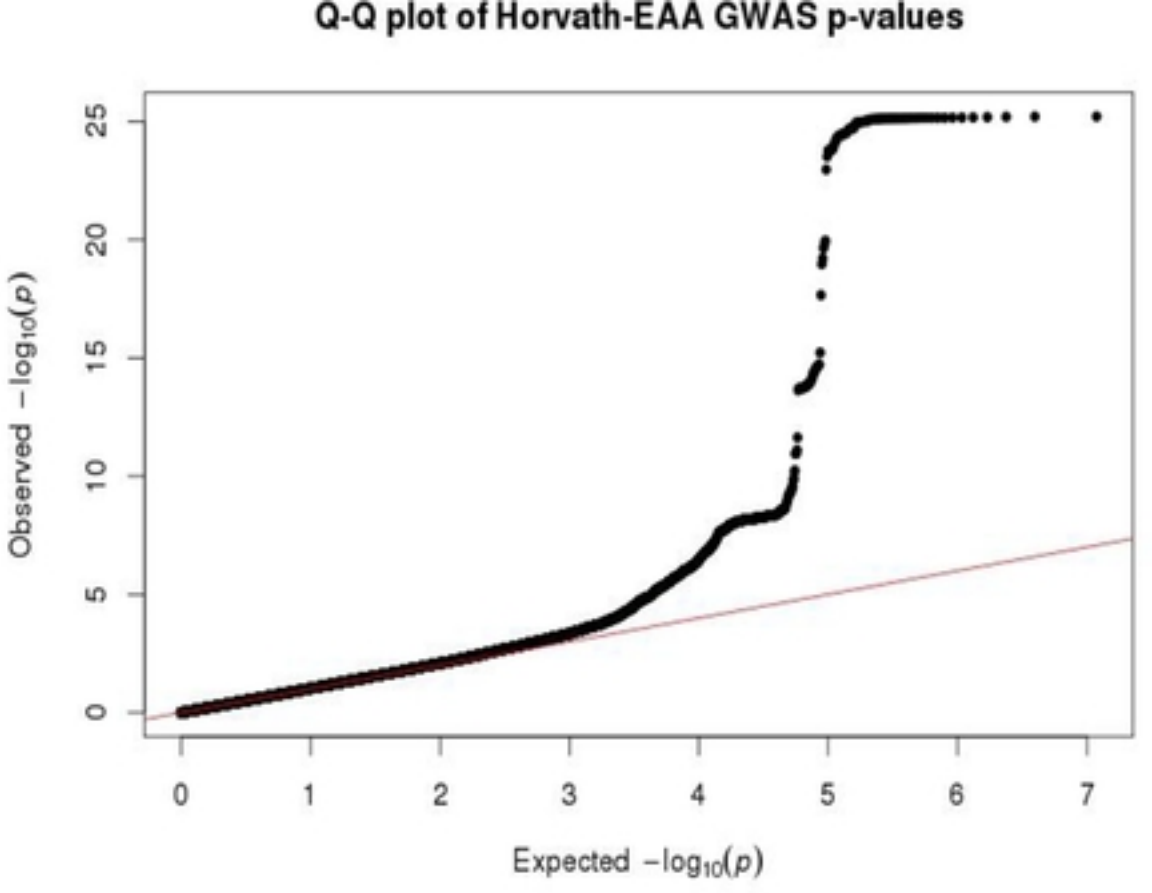
Q-Q plot of Horvath-EAA GWAS p-values
Observed $-\log_{10}(p)$
Expected $-\log_{10}(p)$
0
5
10
15
20
25
0
1
2
3
4
5
6
7

Figure 2